

# Evaluating Fairness in the Presence of Spatial Autocorrelation

Subhabrata Majumdar, Cheryl Flynn, Ritwik Mitra

subho.cbrooks@att.com

Data Science and AI Research, AT&T Chief Data Office

USA

## ABSTRACT

In spite of considerable practical importance, current algorithmic fairness literature lacks in technical methods to account for underlying geographic dependency while evaluating or mitigating fairness issues for spatial data. We initiate the study of spatial fairness in this paper, taking the first step towards formalizing this line of quantitative methods. Fairness considerations for spatial data often get confounded by the underlying spatial autocorrelation. We propose hypothesis testing methodology to detect the presence and strength of this effect, then mitigate it using a spatial filtering-based approach—in order to enable application of existing bias detection metrics. We evaluate our proposed methodology through numerical experiments on real and synthetic datasets, demonstrating that in presence of several types of confounding effects due to the underlying spatial structure our testing methods perform well in maintaining low type-II errors and nominal type-I errors.

## KEYWORDS

fairness, spatial fairness, spatial equity, spatial filtering, hypothesis testing, algorithmic fairness

## 1 INTRODUCTION

With increased mechanization in all corners of life, automated decision-making processes are starting to grapple with massive scale-ups of unfair and prejudicial systems either already present in the society and even some new ones. Fairness concerns have been addressed in machine learning (ML) based criminal justice systems, credit scoring, facial recognition among others. In comparison, fairness in *spatial prioritization* has been studied to a relatively lesser extent. This is owed—in no small measure—to a lack of proper definition of fairness, lack of proper choice of spatial unit, idiosyncrasies associated with spatial data e.g. spatial autocorrelation, not to mention the niche nature of the spatial prioritization problem itself. In this paper, we present the first attempt to formalize a quantitative approach towards problems on spatial fairness.

We focus on spatial fairness through the lens of pre-existing spatial distributions present in a geographic location through localization of different demographic groups in different areas. For historic and societal reasons, distribution of different demographic groups is usually spatially autocorrelated [29]. In this context, we consider deployment of a new service, for example bike share programs, cellular networks, location-based gaming. Such services, especially when deployed through for-profit corporations often are required to adhere to specific fairness guidelines while also attempting to maximize engagement with or subscription to their services. As such, we expect such deployments to track closely with the spatial autocorrelation through demographic features that often act as proxy for net assets and propensity buy/access such

services. Deployment locations of such services may need to be constrained by minimum and maximum distances between adjacent pairs or groups of locations. Potential reasons for imposing such constraints may range from an overall goal for optimal coverage and accessibility (e.g. bikeshare stations), to limitations of the underlying technology (e.g. 5G cellular networks). Our goal is to consider detection of biases that may manifest in such deployments which is substantially more than what would be expected if spatial autocorrelation were the only factor.

*Motivation.* To illustrate the above notion, consider the following scenario. Suppose an organization wants to deploy new service locations (e.g. bikeshare stations) across a city. To do so, its team of analysts has put together a dataset, which consists of pre-designated geographic partitions of the city, whether each partition contains one or more existing service locations ( $Y = 1$  or  $Y = 0$ ), whether that partition is a low-income area or not ( $A = 1$  or  $A = 0$ ), and other input features (denoted by  $X$ )—such as historical demand volume and service quality. By analyzing this data, the team wants to come up with other geographic partitions more amenable to deployment of new service locations, while ensuring that the outcomes are not associated with the income indicator sensitive feature  $A$ .

In the presence of a spatial dependency pattern  $S$  between partitions of a geographic area, the estimation of any association or cause-effect relationship between  $Y$  and  $A$  may be confounded by  $S$ . As demonstrated in the causal diagram in Fig. 1a, there are multiple subcases of the above scenario, which may result in overestimation of the degree of association between  $Y$  and  $A$  through any spurious correlation either or both of them might have with  $S$ .

As a motivating example, consider the 2018 5-year ACS Census data for Cook County, IL, USA. We quantify the spatial dependency pattern  $S$  using a pairwise similarity matrix  $\mathbf{W}$ , consisting of inverse distances between centroids of all pairs of census tracts. We take the percent of population in each census tract that is African American as samples of  $A$ , denoted by  $\mathbf{a} = (a_1, \dots, a_n)^T$ . Using Moran's  $I$  [22], a known measure of spatial autocorrelation, we can conclude that there is significant positive spatial autocorrelation between the entries of  $\mathbf{a}$ , encoded specifically through the pairwise similarities in  $\mathbf{W}$ .

To demonstrate the effect of spurious correlation in this setup, we generate autocorrelated samples of  $Y$

$$\mathbf{x} = (\mathbf{I}_n - \rho\mathbf{W})^{-1}\boldsymbol{\epsilon}; \quad \mathbf{y} = \mathbf{1}(\mathbf{x} > 1), \quad \boldsymbol{\epsilon} \sim N(0, \mathbf{I}_n),$$

and over 1000 realizations of the above observe values of the Kolmogorov-Smirnov (KS) statistic that quantifies the dissimilarity of the conditional distributions  $A|(Y = 0)$  and  $A|(Y = 1)$ . As seen in Fig. 1b, for  $\rho = 0$  (uncorrelated), the conditional distributions are highly similar, as compared to  $\rho = 0.95$  (strong positive spatial autocorrelation). When a hypothesis test (see Section 2.1) is performed at significance level 0.05, the false positive rate is 0.75 for  $\rho = 0.95$ ,

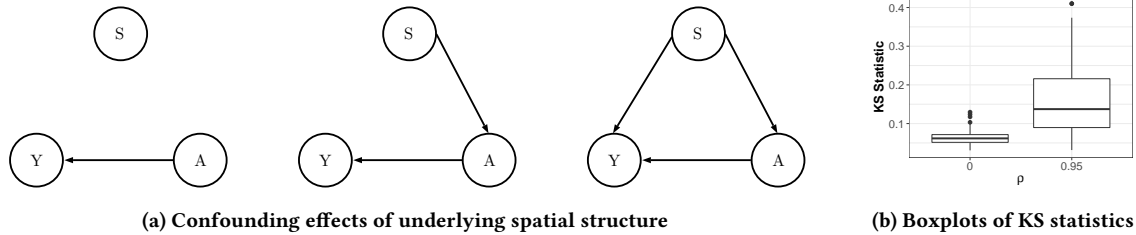


**Figure 1: Detrimental effects of spatial autocorrelation. In presence of spatial autocorrelation, associations between the outcome feature  $Y$  and sensitive feature  $A$  get confounded with potential associations with  $S$  (panel a). This effect translates to inflated values of bias detection metrics in presence of high spatial autocorrelation (panel b).**

compared to only 0.03 for  $\rho = 0$ . This suggests that bias detection methods designed for independent data may have a higher bias detection rates when applied to spatially autocorrelated data directly.

*Related work.* Spatial fairness is an important problem with a myriad of applications that affect the populace in direct and tangible ways. Spatial distribution of resources impact the accessibility (or lack thereof) of crucial private and public goods, such as housing, transportation, schools, and healthcare. Historically, systemic, intentional and even unintentional biases have affected distribution of these resources. The oft-noted illegal practice of ‘redlining’ where credit for housing is often denied to minorities can stem from banks focusing on broad information, such as the neighborhood of the applicant, which ends up disadvantaging those from poorer locations [8]. Fairness concerns in bikeshare problems is well-documented. Ogilvie and Goodman [24] noted inequities in who were accessing London’s Barclays Cycle Hire (BCH) scheme—most users of the system tended to be male and from privileged background; see also [12, 23] and Fig. 2. Availability and access to primary care facilities are essential to the overall well-being of a local community [16]. Spatial inequality in this context has also gotten attention in literature. For example, [18] studied the accessibility and found clear distinctions between rural/poorer and urban/richer areas in Deqing county in China. More recently, evidence has surfaced across multiple geographic areas in the United States regarding racial disparities in COVID-19 vaccine enrollment and distribution attributed to spatial factors [17, 20]. As a final example, [7] found that the popular augmented reality game Pokémon GO disadvantaged urban locations with a higher percentage of minority population, as compared to predominantly white neighborhoods. It is conceivable, that future location-based game developments stemming from the success of Pokémon GO could inherit some of the same racial disparities.

In spite of the very real needs, to the best of our knowledge there are no known methods for detecting and mitigating spatial fairness issues. The study of algorithmic fairness has attracted significant attention in the machine learning community in the past few years. However, most of the methods proposed in this area [21] deal with obtaining *point estimates* of any association of between the outcome  $Y$  and sensitive attribute  $A$ , or mitigating this association while estimating  $Y$ , and not the *significance* of such association. While some very recent methods do propose hypothesis tests for

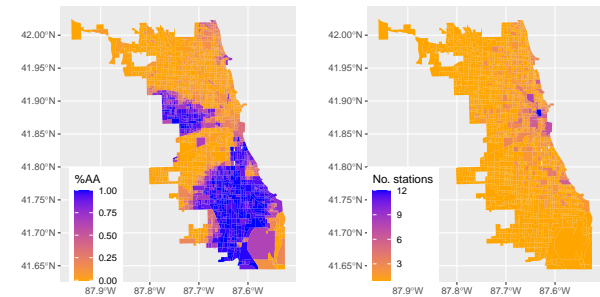


**Figure 2: Spatial distribution of bikeshare stations in Chicago (left) is largely complementary to that of the percentage of African Americans (right) at census tract level.**

evaluating fairness [5, 9], they assume the data samples analyzed to be independent. As we have seen in the motivating example, the presence of an underlying dependency pattern can result in such tests conflating this dependence with the presence of actual demographic bias.

*Our contributions.* In this paper, we provide a methodological framework for the evaluation of fairness concerns in spatial data, specifically in the scenarios when confounding effects of spatial autocorrelation influence the outcomes of interest, or the sensitive attribute values, or both. Under this setup, we aim to evaluate a number of scenarios regarding the effect of an underlying spatial structure. These scenarios concern the detection of a common spatial effect, detection of whether these effects are equivalent in magnitude, and finally testing for association between the underlying feature  $Y$  and sensitive feature  $A$  while adjusting for this spatial effect. We formalize the above using a number of research questions (see Section 3), and propose hypothesis testing methods that provide answers to them. We evaluate these methods in a number of data settings, including the Chicago bikeshare data in Fig. 2.

## 2 PRELIMINARIES

We introduce a few concepts before diving deeper into our fairness evaluation methods. Consider  $n$  location units given by  $\{l_i\}_{i=1}^n$ . For each location unit  $i$ , we have a set of features  $X_i \in \mathbb{R}^p$  that carry information regarding the characteristics of the said location unit.

This gives rise to data matrix  $\mathbf{X} = (\mathbf{X}_1, \dots, \mathbf{X}_n)^T \in \mathbb{R}^{n \times p_1}$ . Additionally, we have a (binary or continuous) response variable  $\mathbf{y} \in \mathbb{R}^n$  that indicates whether a certain resource is allocated to the location  $i$ . In practice, this response may be the indicator of any presence of a resource in the said location. Define  $\mathbf{A} = (\mathbf{A}_1, \dots, \mathbf{A}_n)^T \in \mathbb{R}^{n \times p_2}$  which contains the corresponding sensitive features. We define  $D_i = (y_i, \mathbf{X}_i, \mathbf{A}_i)$  as the data unit of the  $i^{\text{th}}$  observational unit. For each random vector, we use their lowercase counterpart to represent their realized value; e.g. for  $\mathbf{X}_i$ , we use  $\mathbf{x}_i$  to represent its realization and so on. For simplicity, we state our methods assuming a single sensitive attribute  $A$ , i.e.  $p_2 = 1$ .

## 2.1 Hypothesis testing

Statistical hypothesis testing is a way to determine whether the results obtained from analyzing a dataset provide meaningful evidence towards a certain hypothesis on the underlying process generating that data. The null hypothesis ( $H_0$ ) represents a default assumption on the data generating process, which is tested against the alternative hypothesis ( $H_a$ ). For this comparison, a *test statistic* is calculated from the data, and if the statistic value falls outside an interval, the test rejects  $H_0$  in favor of  $H_a$ . Hypothesis tests can be seen as a decision function  $\phi(\cdot)$  that takes a dataset  $\mathcal{D}$  as input, and given a significance level  $1 - \alpha$ ,  $\alpha \in (0, 1)$ , along with hypotheses  $H_0, H_a$ , returns the decision whether to reject  $H_0$  in favor of  $H_a$  or not. Two types of errors can happen in this decision problem: (1) Type-I error, or the error of rejecting  $H_0$  based on the data when it is true in reality, and (2) Type-II error, or the error of failing to reject  $H_0$  when it is actually false. A good test would ideally have both errors small. Generally, in hypothesis problems a hard constraint on the upper bound of the type-I error is imposed:

$$\Pr[\phi(\mathcal{D}; \alpha) = \text{Reject } H_0 | H_0 \text{ is true}] \leq \alpha,$$

where the probability is calculated over the randomness of the data.

Given sample data, a *test statistic*  $T$  is calculated to take the above decision  $\phi$ . A  $p$ -value refers to the probability that  $T$  is at least as extreme (as high or low, depending on what  $H_a$  is) as  $t$ —the value of  $T$  for the sample data—given that  $H_0$  is true. When  $p$ -value is  $\leq \alpha$ , we take the decision  $\phi(\mathcal{D}; \alpha) = \text{Reject } H_0$ , else  $\phi(\mathcal{D}; \alpha) = \text{do not reject } H_0$ . To calculate the  $p$ -value, we need access to the null distribution of  $T$ . Depending on the test, this is obtained either using known asymptotic results, or approximated using permutation or bootstrap.

## 2.2 Testing for spatial autocorrelation

Moran’s I [22] is a well-known statistic to test for global dependence in spatial datasets. Given realizations of a continuous random variable  $Z$ , say  $\mathbf{z} = (z_1, \dots, z_n)^T$ , and a weight matrix  $\mathbf{W} = ((w_{ij}))$ , Moran’s I is formally defined as

$$I = \frac{n}{\bar{w}} \frac{\sum_{i=1}^n \sum_{j=1}^n w_{ij} (y_i - \bar{y})(y_j - \bar{y})}{\sum_{i=1}^n (y_i - \bar{y})^2},$$

where  $\bar{w} = \sum_{i,j} (w_{ij} + w_{ji})/2$ ,  $\bar{y} = \sum_i y_i/n$ . Under the null hypothesis that no spatial autocorrelation exists, a centered and scaled version of  $I$  is asymptotically standard Gaussian [25, 28]. Recently, Lee and Ogburn [19] generalized the Moran’s I for realizations of a categorical random variable  $Z^*$  (denote by  $\mathbf{z}^*$ ), and proposed an

analogous test statistic:

$$\Phi = \frac{n}{W} \sum_{i=1}^n \sum_{j=1}^n \frac{2w_{ij} [\mathbb{I}(z_i^* = z_j^*) - 1]}{P(Z^* = z_i^*)P(Z^* = z_j^*)}.$$

When observations are binary, standardized versions of Moran’s I and the  $\Phi$  statistic above are equivalent, and asymptotically standard Gaussian [19]. Asymptotic Gaussian tail-bounds or permutation tests can be used to obtain  $p$ -values of either test statistic.

## 2.3 Eigenvector Spatial Filtering

Eigenvector Spatial Filtering (ESF) [10, 13, 15] is a popular method to remove underlying spatial dependencies from spatial observations. It fits a linear regression on that feature, using the top few eigenvectors of the weight matrix  $\mathbf{W}$  and a number of covariates as input features. The residuals from this regression can be used as dependency-free analogues of the original observations for further analysis.

Formally, this *spatial autoregression* model assumes:

$$\mathbf{y} = (\mathbf{I}_n - \rho \mathbf{W})^{-1} (\mathbf{X} \boldsymbol{\beta} + \boldsymbol{\epsilon}); \quad \boldsymbol{\epsilon} \sim N(0, \sigma^2 \mathbf{I}_n), \sigma > 0.$$

where  $\rho \in [-1, 1]$  denotes the degree of spatial autocorrelation, and  $\boldsymbol{\beta} \sim \mathbb{R}^p$  quantifies the (linear) effect of the covariates  $\mathbf{X}$  on  $Y$ . Given that the spatial dependency in  $Y$  is entirely due to the top  $k$  few eigenvectors of  $\mathbf{W}$ , Consider now the spectral decomposition  $\mathbf{W} = \mathbf{E} \boldsymbol{\Lambda} \mathbf{E}^T$ , where  $\mathbf{E} \in \mathbb{R}^{n \times n}$  is orthogonal and  $\boldsymbol{\Lambda} \in \mathbb{R}^{n \times n}$  is diagonal. Using straightforward algebra [15], the above model simplifies to

$$\begin{aligned} \mathbf{y} &= \rho \mathbf{E} \boldsymbol{\Lambda} \mathbf{E}^T \mathbf{y} + \mathbf{X}^T \boldsymbol{\beta} + \boldsymbol{\epsilon} \\ &\simeq \rho \mathbf{E}_k \boldsymbol{\gamma}_k + \mathbf{X}^T \boldsymbol{\beta} + \boldsymbol{\zeta}, \end{aligned} \quad (1)$$

where  $\boldsymbol{\gamma}_k$  estimates the effect of the top  $k$  eigenvectors, and  $\boldsymbol{\zeta} \sim N(0, \sigma_1^2 \mathbf{I}_n)$ ,  $\sigma_1 > 0$ . The least square estimates of  $\boldsymbol{\gamma}_k, \boldsymbol{\beta}$  can be plugged in to obtain a ‘sanitized’, decorrelated version of  $\mathbf{y}$ :

$$\tilde{\mathbf{y}} = \mathbf{y} - \rho \mathbf{E}_k \hat{\boldsymbol{\gamma}}_k + \mathbf{X} \hat{\boldsymbol{\beta}}.$$

In practice, the number of eigenvectors required to perform this filtering,  $k$ , is unknown, and model selection or sparse penalization methods [27] may be used to obtain an optimal subset of eigenvectors in Eq. (1).

## 2.4 Fairness metrics

A number of metrics have been proposed in the algorithmic fairness literature that detect demographic bias, for example disparate impact, demographic parity, and statistical parity [21]. Many of these have been proposed keeping classification problems in mind, and work for binary sensitive attribute  $A$ , and either discrete labels  $Y$  or probabilistic outputs  $\hat{Y}$ . For example, the disparate impact (DI) metric calculates the ratio of positive probabilities given different values of the sensitive attribute:

$$\text{DI}(Y, A) = \frac{\Pr(Y = 1 | A = 1)}{\Pr(Y = 1 | A = 0)}.$$

When one or more of  $Y, A$  is continuous, standard statistical tests like the KS statistic, or  $t$ -tests can be used to distinguish between the distributions of the continuous attribute, conditioned on different values of the discrete attribute. Finally, when both  $Y$  and  $A$  are continuous, methods to correlate samples of continuous random

variables, such as the Pearson's (linear) correlation coefficient and Spearman's rank correlation can be used.

### 3 METHODOLOGY

Under the setup of Section 2, we aim to answer three questions: (Q1) Are both  $Y$  and  $A$  significantly associated with the common weight matrix  $\mathbf{W}$ ? (Q2) Given that they both exhibit significant association with  $\mathbf{W}$ , are their strength of associations with  $\mathbf{W}$  similar? (Q3) Can we adjust for spatial association to measure the true degree of association between  $Y$  and  $A$ ? To answer the first two questions, we adapt a combination hypothesis testing procedure based on the Moran's I statistic. For the third question, we use ESF to eliminate any spatial dependency in  $Y$  and/or  $A$ .

#### 3.1 Testing for common autocorrelation

Assume that the standardized Moran's I calculated using the size- $n$  sample  $\mathbf{y}$  (or  $A$ ) and  $\mathbf{W}$  follow the (non-asymptotic) location family distribution  $F(\cdot, \mu_y)$  (or  $F(\cdot, \mu_a)$ ) with mean parameter  $\mu_y$  (or  $\mu_a$ ). Then, to answer the question (Q1) above, we test the following:

$$H_{0y}^1 : \mu_y = 0 \quad \text{vs.} \quad H_{ay}^1 : \mu_y \neq 0 \quad \text{and} \\ H_{0j}^1 : \mu_a = 0 \quad \text{vs.} \quad H_{aa}^1 : \mu_a \neq 0.$$

Specifically, we are interested in knowing whether the scenario when both the alternate hypotheses hold, i.e. both  $y$  and  $A$  exhibit significant autocorrelation. Thus we test for the combined null  $H_0^1 = H_{0y}^1 \cup H_{0a}^1$  against the combined alternative  $H_a^1 = H_{ay}^1 \cap H_{aa}^1$ . Similarly, to answer question (Q2), we test  $H_0^2 = H_0^{21} \cup H_0^{22}$  against  $H_a^2 = H_a^{21} \cap H_a^{22}$ , where

$$H_0^{21} : \mu_y - \mu_a \geq \delta \quad \text{vs.} \quad H_a^{21} : \mu_y - \mu_a < \delta \quad \text{and} \\ H_0^{22} : \mu_y - \mu_a \leq -\delta \quad \text{vs.} \quad H_a^{22} : \mu_y - \mu_a > -\delta,$$

for some fixed  $\delta > 0$ , and with the additional assumption that  $\mu_y \neq 0, \mu_a \neq 0$ . Guidance for useful values of  $\delta$  may be determined by target thresholds of fairness metrics, such as the disparate impact thresholds of (0.8, 1.2) based on the EEOC four-fifths rule [11]. We take  $\delta = 1$  in our experiments to account for small differences that may occur under null between the two standardized Moran's I statistics due to sampling noise.

The above setup is different from traditional multiple testing, where a common null is evaluated against multiple alternatives, and is known as the Intersection-Union (IU) principle [3, 4]. Working under the IU principle, we combine test statistics for each of the pairs of sub-hypotheses above using the concept of *Pivotal Parametric Products*:

**Definition 3.1** ([26]). For the problem of testing for a (possibly vector-valued) parameter  $\theta$  using a union null  $H_0 \equiv \bigcup_{s=1}^S H_{0s}$ , a Pivotal Parametric Product (P3) is defined as any function  $\eta \equiv g(\theta)$  such that  $H_0$  holds if  $\eta = 0$ .

Consequently, testing for  $H_0 : \eta = 0$  can be done using an (unbiased or consistent) estimator of  $\eta$ . In our context, we define the P3 functions to test for  $H_0^1$  vs.  $H_a^1$  and  $H_0^2$  vs.  $H_a^2$  as:

$$P_1 = \min(|\mu_y|, |\mu_a|); \quad P_2 = |(\mu_y - \mu_a)^2 - \delta^2|.$$

Assuming that the individual Moran's I test statistics are called  $I_y$  and  $I_a$ , respectively for  $y$  and  $A$ , the corresponding test statistics will be:

$$T_1 = \min(|I_y|, |I_a|); \quad T_2 = |(I_y - I_a)^2 - \delta^2|.$$

Denoting the lower- $p$  ( $p \in [0, 1]$ ) tail of the probability distribution of a statistic  $T$  by  $T_p$ , rejection regions at level  $\alpha$  for the above tests are characterized by large values of  $T_1$  and small values of  $T_2$ , specifically by the sets  $\{T_1 \geq T_{1,1-\alpha}\}$  and  $\{T_2 \leq T_{2,\alpha}\}$ , respectively.

Practically, the first test rejects the composite null at level  $\alpha \in [0, 1]$  only if *both* individual Moran's I statistics are above a certain  $\alpha' \in [0, 1]$ . One option of combining the two individual level- $\alpha'$  tests to get a level- $\alpha$  composite test here is to just take  $\alpha' = \alpha$  [3]. But this option tends to highly conservative in maintaining the nominal level of the overall test, meaning that under practical data generating situations, the empirical type-I error tends to be much lower than the upper bound of  $\alpha$  [4].

We use permutation testing to navigate the above difficulties. We construct the null distributions for each test statistic by calculating them over randomly permuted samples, then compute the tail probabilities of the statistics above with respect to the respective distributions. The steps are as follows:

- Suppose  $\Pi_n$  is the set of all permutations of  $\{1, \dots, n\}$ . For some permutation  $\pi \in \Pi_n$ , we calculate the Moran's I statistics from permuted samples, say  $I_{y,\pi}, I_{j,\pi}$ , and using these the P3 test statistics  $T_{1,\pi}, T_{2,\pi}$ .
- Given some large integer  $M$ , we obtain permuted samples of the test statistics under their respective null hypotheses by repeating the above for random permutations  $\pi_1, \dots, \pi_M$ :

$$\mathcal{T}_1^0 = \{T_{1,\pi_1}, \dots, T_{1,\pi_M}\}; \quad \mathcal{T}_2^0 = \{T_{2,\pi_1}, \dots, T_{2,\pi_M}\}.$$

- The permutation  $p$ -values are empirical tail probabilities of  $T_1, T_2$  corresponding to the respective (empirical) null distributions:

$$\hat{p}_1 = \frac{1}{M} \sum_{m=1}^M \mathbb{I}(T_{1,\pi m} \geq T_1), \\ \hat{p}_2 = \frac{1}{M} \sum_{m=1}^M \mathbb{I}(T_{2,\pi m} \geq T_2).$$

Note that in order to generate the joint null distribution of  $(T_1, T_2)$ , it is important to use the *same* set of permutations  $\pi_i$  to generate null samples  $\mathcal{T}_1^0$  and  $\mathcal{T}_2^0$  above [1].

#### 3.2 ESF adjustment

To address (Q3) above, i.e. adjusting for underlying autocorrelation while testing for true bias, we use ESF to learn features that capture the spatial structure in  $Y$  and  $A$ . We then use these features to adjust the bias detection procedure. As described in Section 2.3, when the feature being analyzed is continuous, its decorrelated version is obtained using residuals from its spatial autoregression. We use  $\ell_1$ -penalization to automatically choose the best subset of eigenvector while estimating the ESF coefficients:

$$(\hat{\mathbf{y}}_k, \hat{\boldsymbol{\beta}}) = \operatorname{argmin}_{\mathbf{y}, \boldsymbol{\beta}} \left[ \frac{1}{2n} \|\mathbf{y} - \rho \mathbf{E} \mathbf{y} - \mathbf{X} \boldsymbol{\beta}\|^2 + \lambda \|\mathbf{y}\|_1^2 \right], \\ \tilde{\mathbf{y}} = \mathbf{y} - \rho \mathbf{E}_k \hat{\mathbf{y}}_k + \mathbf{X} \hat{\boldsymbol{\beta}}.$$

To choose the tuning parameter  $\lambda$  in the above optimization procedure, we use two methods: Akaike Information Criterion (AIC) and Bayesian Information Criterion (BIC). We train separate models for a range of  $\lambda$  values, and choose the model with the minimum values for either AIC or BIC.

When the feature being analyzed is discrete, we use an autologistic model [14], which is simply a logistic version of the spatial autoregression model discussed. Thus, we estimate  $\boldsymbol{\gamma}$ ,  $\boldsymbol{\beta}$  from the below model, again using  $\ell_1$ -penalization to select the number of eigenvectors of  $\mathbf{E}$ :

$$p_{yi} := \Pr(y_i = 1 | \mathbf{E}, \mathbf{y}, \mathbf{X}) \\ = [1 + \exp\{-(\rho \mathbf{E} \boldsymbol{\gamma} + \mathbf{X} \boldsymbol{\beta})\}]^{-1}; \quad i = 1, \dots, n.$$

There are now three possible cases: both  $Y, A$  are continuous, both are discrete, or one of them is continuous and the other is discrete. Below we describe ESF-adjusted testing strategies for each of these cases. In each case, we denote a generic bias metric computed before and after ESF by  $r(\cdot, \cdot)$ .

*Case I: both continuous.* Examples of relevant fairness metrics in this situation are Pearson's correlation coefficient, Spearman's rank correlation, and Kendall's Tau. In this case, the post-ESF bias metric is computed by simply using the respective residuals, i.e.  $r(\hat{\mathbf{y}}, \hat{\mathbf{a}})$  in place of  $r(\mathbf{y}, \mathbf{a})$ , and compared against standard thresholds for that metric.

*Case II: both discrete.* Disparate impact, equalized odds, and equality of opportunity are examples of fairness metrics applicable when both  $Y, A$  are discrete. In our setting, we first estimate the sample-level probabilities using ESF:

$$\hat{p}_{yi} = [1 + \exp\{-(\rho \mathbf{E}_{ky} \hat{\boldsymbol{\gamma}}_{ky} + \mathbf{X} \hat{\boldsymbol{\beta}}_y)\}]^{-1}, \\ \hat{p}_{ai} = [1 + \exp\{-(\rho \mathbf{E}_{ka} \hat{\boldsymbol{\gamma}}_{ka} + \mathbf{X} \hat{\boldsymbol{\beta}}_a)\}]^{-1}; \quad i = 1, \dots, n.$$

Following this, we generate  $\hat{\mathbf{y}}_i^b \sim \text{Bernoulli}(\hat{p}_{yi})$ ,  $\hat{\mathbf{a}}_i^b \sim \text{Bernoulli}(\hat{p}_{ai})$ , and calculate  $r(\hat{\mathbf{y}}^b, \hat{\mathbf{a}}^b)$ . We repeat this  $B$  times, and obtain the collection of metrics  $\{r(\hat{\mathbf{y}}^b, \hat{\mathbf{a}}^b) : b = 1, \dots, B\}$ —fixing  $B = 1000$  in our experiments. This simulates the empirical null distribution of the bias metric, i.e. under the assumption that the only bias present in the data is due to  $\mathbf{W}$ . We now simply compare the unadjusted metric against this distribution to obtain an approximate  $p$ -value:

$$\hat{p} = \frac{1}{B} \sum_{b=1}^B \mathbb{I}(r(\hat{\mathbf{y}}^b, \hat{\mathbf{a}}^b) \geq r(\mathbf{y}, \mathbf{a})).$$

*Case III: one discrete, one continuous.* The KS statistic is an example metric that can be used when one of  $Y, A$  is discrete. In this situation, we simply estimate the sample class probabilities for the discrete feature (without loss of generality,  $Y$ ) and approximate the empirical null distribution of bias metrics using multiple simulated copies of the ESF-adjusted  $\hat{\mathbf{y}}$  and the fixed, continuous fitted values  $\hat{\mathbf{a}}$ :  $\{r(\hat{\mathbf{y}}^b, \hat{\mathbf{a}}) : b = 1, \dots, B\}$ . The  $p$ -value is simply the tail probability at  $r(\mathbf{y}, \mathbf{a})$  with respect to this empirical distribution.

## 4 NUMERICAL EXPERIMENTS

To evaluate our hypothesis testing methods, we consider the following experimental setup. We take the centroid locations of  $n = 2080$

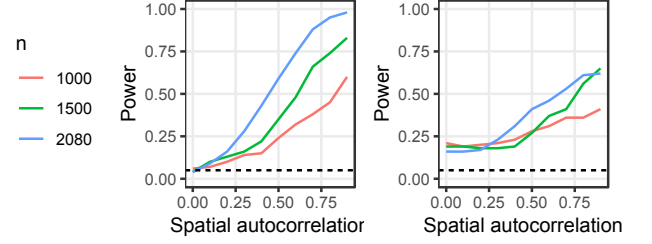


**Figure 3: Powers for  $T_1$  (left) and  $T_2$  (right) under association and correlation. Dotted lines indicate size  $\alpha = 0.05$ .**

census block groups in the city of Chicago, construct a weight matrix  $\mathbf{W}$  using the inverse of distances between tracts  $i, j$  as the weight  $w_{ij}$ ,  $1 \leq i, j \leq n$ , and generate samples of the random variables  $(Y, \mathbf{X}, \mathbf{a})$  some or all of which are spatially autocorrelated. Under this basic setup, we consider a number of settings that cover a number of possible scenarios. When required, we use 1000 permutations to generate approximate null distributions, and compute all empirical rejection rates using 1000 Monte Carlo runs.

### 4.1 Testing for common autocorrelation

We evaluate the performance of the IU-combination tests in the three different scenarios described in Fig. 1.

*4.1.1 Association by autocorrelation.* We first focus on the case where both the response  $Y$  and the sensitive attribute  $A$  are independently correlated with  $\mathbf{W}$ . We start with standard Gaussian errors  $\boldsymbol{\epsilon}_1, \boldsymbol{\epsilon}_2 \sim N(0, \mathbf{I}_n)$ , and given a value of spatial autocorrelation  $\rho$ , generate the spatially lagged features:

$$\mathbf{y} = (\mathbf{I} - \rho \mathbf{W})^{-1} \boldsymbol{\epsilon}_1, \quad \mathbf{a} = (\mathbf{I} - \rho \mathbf{W})^{-1} \boldsymbol{\epsilon}_2.$$

We repeat the experiment for  $\rho = 0, 0.1, \dots, 0.9$ , and different sample sizes, by either randomly choosing 1000 and 1500 census tracts or using all 2080 census tracts, to quantify how the degree of spatial autocorrelation and sample size affect the power (i.e. Type-II error) of the testing procedure.

We summarize the results in Fig. 3. As the degree of spatial autocorrelation  $\rho$  increases, the testing procedure is able to detect the existence of a non-zero  $\rho$  with higher power. The test also maintains nominal size, as the value of  $T_1$  is exactly 0.05 for  $\rho = 0$ . For  $T_2$ , note that rejection implies inferring the equality of  $\rho$  across  $\mathbf{y}$  and  $\mathbf{a}$ . Thus Figure 3 indicates that our permutation test is also able to infer this with higher power as  $\rho$  grows larger. The values at  $\rho = 0$  indicates that the test  $T_1$  is well-calibrated, i.e. maintains nominal size ( $\alpha = 0.05$ ) in absence of any signal. Note that for  $T_2$  the alternate hypothesis implies inferring the equality of spatial autocorrelation. This is the case here, so the test rightly maintains rejection rates above 0.05 for all values of  $\rho$ . Finally, increasing sample size has a positive effect in the performance of both tests.

*4.1.2 Association and autocorrelation.* In this situation  $Y$  and  $A$  are associated independently, and one or both are spatially autocorrelated. To represent such scenario, we generate synthetic data using the two settings, starting with start with standard Gaussian errors

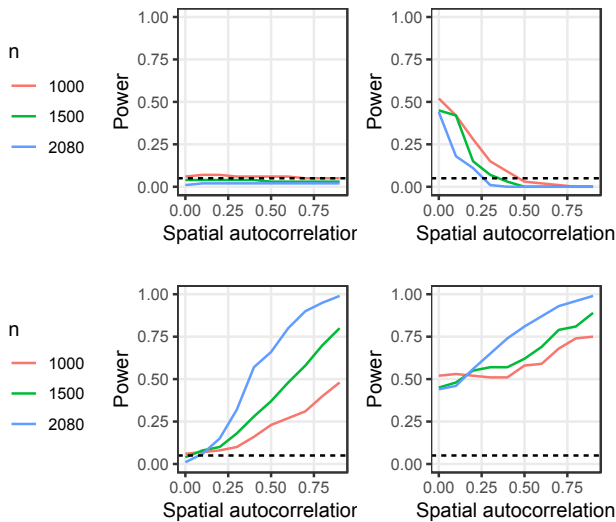


**Figure 4: Powers for  $T_1$  (left) and  $T_2$  (right) under association and correlation. Top and bottom rows correspond to settings (2) and (3), respectively.**

$\epsilon_1, \epsilon_2$  as before:

$$\mathbf{a}_0 = \epsilon_2, \mathbf{y} = 5\mathbf{a}_0 + \epsilon_1, \mathbf{a} = (\mathbf{I} - \rho\mathbf{W})^{-1}\mathbf{a}_0, \quad (2)$$

and

$$\mathbf{a} = (\mathbf{I} - \rho\mathbf{W})^{-1}\epsilon_2, \mathbf{y} = 5\mathbf{a} + \epsilon_1. \quad (3)$$

In the first case only the sensitive attribute is spatially autocorrelated, while in the second situation both  $Y$  and  $A$  are.

We summarize the results in Fig. 4. The statistic  $T_1$  geared towards finding evidence of a common level of spatial autocorrelation (rightly) maintains nominal size across different values of  $\rho$  in the first case above, and increasingly becomes more powerful for higher  $\rho$  in the second case. The statistic  $T_2$  maintains nominal rejection rates for moderate to high  $\rho$  in the first case, giving evidence that there is a mismatch of autocorrelation magnitudes for  $Y$  and  $A$ . In the second case, it however maintains higher rejection rates.

**4.1.3 Proxy autocorrelation.** We now consider the third scenario, of  $Y$  being associated with *non-sensitive* attributes, i.e. components of  $X$ , but not  $A$ . However  $X$  and  $A$  are spatially autocorrelated with the same  $\mathbf{W}$ .

$$\mathbf{x} = (\mathbf{I} - \rho\mathbf{W})^{-1}\epsilon_2, \mathbf{y} = 5\mathbf{x} + \epsilon_1; \quad \mathbf{a} = (\mathbf{I} - \rho\mathbf{W})^{-1}\epsilon_2.$$

The results for this setting (not shown) are very similar to Fig. 3. This is because setting 3 can be seen as the noisy version of setting 1, where we were essentially testing for a common source of autocorrelation between  $\mathbf{x}$  and  $\mathbf{a}$ , as compared to  $\mathbf{y}$  and  $\mathbf{a}$  here.

## 4.2 Adjusting for autocorrelation

For this experiment, we consider two different values of the underlying spatial autocorrelation, and evaluate the ESF-based testing methods for discrete and continuous attributes across the above settings.

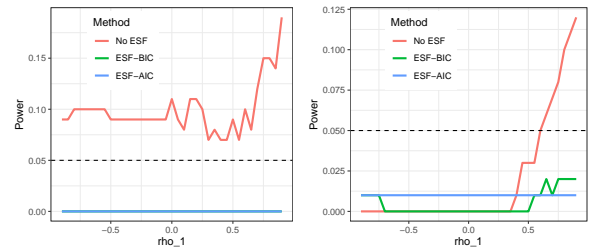


**Figure 5: Rejection rates for the ESF-adjusted tests under association by autocorrelation, when  $Y, A$  are (left) both continuous, or (right) both discrete.**

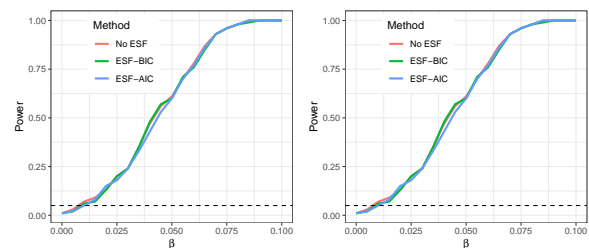


**Figure 6: Rejection rates for the ESF-adjusted tests under association and autocorrelation, when both  $Y, A$  are discrete.**

**4.2.1 Association by autocorrelation.** For the continuous setup, we consider the model

$$\mathbf{y} = (\mathbf{I} - \rho_1\mathbf{W})^{-1}\epsilon_1, \quad \mathbf{a} = (\mathbf{I} - \rho_2\mathbf{W})^{-1}\epsilon_2,$$

and compare error rates of asymptotic tests using the correlation coefficient before and after ESF-adjustment. For the discrete setup, we take  $\mathbf{y} \leftarrow \mathbb{I}(\mathbf{y} > 0), \mathbf{a} \leftarrow \mathbb{I}(\mathbf{a} > 0)$ , and compare using the disparate impact metric. In this case we obtain the null distribution using a permutation procedure. In both cases, we consider the range of values  $\rho_1 = 0.9, \rho_2 = -0.9, -0.85, \dots, 0.85, 0.9$ .

We summarize the results in Fig. 5, with two choices of eigenvector selection using ESF—using AIC and BIC. Without the ESF correction, rejection rates stay above the nominal 0.05 level across all values of  $\rho_2$ . However, after spatial filtering is applied, the rejection rates come down to below nominal level.

**4.2.2 Association and autocorrelation.** In this setup, we consider the case when both  $Y, A$  are discrete. We consider the two subcases:

$$\mathbf{a}_0 = \epsilon_2, \mathbf{y} = \mathbb{I}(\beta\mathbf{a}_0 + \epsilon_1 > 0), \mathbf{a} = \mathbb{I}((\mathbf{I} - \rho\mathbf{W})^{-1}\mathbf{a}_0 > 0),$$

and

$$\mathbf{a} = \mathbb{I}((\mathbf{I} - \rho\mathbf{W})^{-1}\epsilon_2 > 0), \mathbf{y} = \mathbb{I}(\beta\mathbf{a} + \epsilon_1 > 0).$$

We present the results in Fig. 6, calculated on a range of values for  $\beta$ , and fixing  $\rho = 0.9$ —with outputs for the first case on the left and second case on the right. It is evident from the results that the rejection rates remain the same pre- and post-filtering.

**4.2.3 Proxy autocorrelation.** The results due to proxy autocorrelation are largely similar to the first setting, *Association by autocorrelation*, so we omit those results.

## 5 CHICAGO BIKESHARE DATA

We apply our methodology on the Chicago bikeshare data<sup>1</sup>, which contains latest information on the location and other neighborhood-related attributes of all bikeshare stations in the city of Chicago. We join this data with the 2018 ACS Census data to obtain two sensitive features at census tract level—percentage of African American population (%AA), and median income. The comparative plots of bikeshare stations vs. %AA (Fig. 2) presents evidence of potential spatial fairness issues in this context. We perform Moran’s I-based tests for a number of categorical and continuous variables to determine their dependence on the weight matrix  $W$ . We consider several choice of  $W$ : spatial cross-covariance matrices with exponential covariance function having scaling parameters  $10^i$ ;  $i = 0, -1, -2, -3$ , and adjacency matrices indicating 1-hop and 2-hop neighbors of block groups. Results are summarized in Table 1. So this table shows that both sensitive features and the response variable are spatially auto-correlated. Based on the above single-feature Moran’s I, the IU combination test statistics  $T_1$  calculated turns out to be significant for all sensitive features, but  $T_2$  does not. This demonstrates the presence of a common spatial factor, but the magnitudes of such effects are not the same for the bikeshare indicator vs. any of the sensitive features considered.

We perform ESF on three census tract-level features: number of bikeshare stations, %AA, and median income, based on eigenvectors of the inverse-distance weighted  $W$ . Table 2 shows the results from pairwise significance tests based on correlations test before and after removing spatial effects using ESF. Without applying ESF the tests conclude significant association between each of the two sensitive features and bikeshare station numbers in a census tract. However, the underlying spatial autocorrelation completely accounts for this association, and the ESF-adjusted features do not show any significant correlation. Interestingly, the two sensitive features are associated with each other, even after ESF, as is evident by the last row of Table 2.

In the ESF procedure, eigenvectors 3 and 4 were selected in the set of autoregressed eigenvectors for all three features. Looking at the projections of each of the 3 features analyzed along these eigenvectors (Fig. 7), we see that the spatial patterns are largely similar. This underlines the confounding effect of a common spatial factor on our features under consideration.

## 6 CONCLUSION

In this paper, we have presented a methodological approach for evaluating spatial fairness concerns. As demonstrated through examples and real data situations, the influence of a common spatial factor may have a confounding effect on the estimation and evaluation of any association between a demographically sensitive feature and an outcome of interest. Our proposed hypothesis testing methods provide a first set of quantitative tools to tackle this problem. Even though spatial equity and accessibility has received attention in the geospatial data analysis literature [2, 6], this attention has not yet carried over to the algorithmic fairness, or the ML community in general. We aim to bridge this gap through our paper, and foster new developments in this very relevant domain.

<sup>1</sup><https://data.cityofchicago.org/Transportation/Divvy-Trips/fg6s-gzgv>

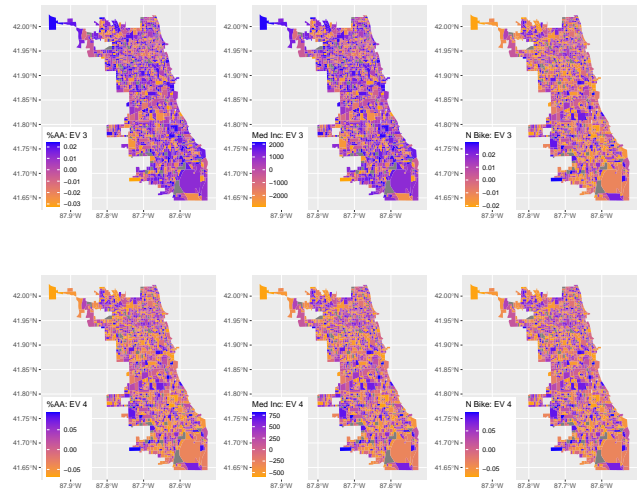


**Figure 7: Projections along the third (top row) and fourth eigenvectors (bottom row) of  $W$ , for the analyzed features.**

An immediate line of future research is the conceptualization of methods to *mitigate* detected spatial fairness issues. It is not enough to ensure that the deployment of a spatially-based service has no source of bias apart from the underlying spatial factor. This may perpetuate underlying inequity structures and skew distribution of resources further away from disadvantaged communities. To this end, a bi-level mitigation may be necessary—mitigating both sources of demographic bias in the outcome of a ML-based deployment prioritization model, with *and* without consideration to the underlying spatial structure. Compared to the numerous existing bias mitigation methods for independent data, this imposes a harder constraint on the underlying utility maximization problem.

We note that methodology similar to ours may be applicable to other dependent data problems as well—such as mixed effect models, and analysis of covariate data attached to nodes in networks—contingent on assumptions relevant for the specific class of problems under consideration.

## REFERENCES

- [1] R. Arboretti, E. Carrozzo, F. Pesarin, and L. Salmaso. 2018. Testing for equivalence: an intersection-union permutation solution. *Stat. Biopharm. Res.* 10 (2018), 130–138.
- [2] Fajle Rabbi Ashik, Sadia Alam Mim, and Meher Nigar Neema. 2020. Towards vertical spatial equity of urban facilities: An integration of spatial and aspatial accessibility. *Journal of Urban Management* 9, 1 (2020), 77–92.
- [3] R.L. Berger. 1982. Multiparameter hypothesis testing and acceptance sampling. *Technometrics* 24 (1982), 295–300.
- [4] R. L. Berger and J. C. Hsu. 1996. Bioequivalence trials, intersection-union tests and equivalence confidence sets. *Stat. Sci.* 11 (1996), 283–319.
- [5] E. Black, S. Yeom, and M. Fredrikson. 2020. FlipTest: fairness testing via optimal transport. In *FAT\*–2020*. 111–121.
- [6] Casey D. Cobb. 2020. Geospatial Analysis: A New Window Into Educational Equity, Access, and Opportunity. *Review of Research in Education* 44, 1 (2020), 97–129.
- [7] Ashley Colley, Jacob Thebault-Spieker, Allen Yilun Lin, Donald Degraen, Benjamin Fischman, Jonna Häkkinen, Kate Kuehl, Valentina Nisi, Nuno Jardim Nunes, Nina Wenig, et al. 2017. The geography of Pokémon GO: beneficial and problematic effects on places and movement. In *Proceedings of the 2017 CHI Conference on Human Factors in Computing Systems*. 1179–1192.

W	$\mathbb{I}(\text{no. stations} \geq 1)$	%AA	Med. inc.	$\mathbb{I}(\%AA \geq 30)$	$\mathbb{I}(\text{Med. inc.} \geq 50k)$
Exp, $V = 1$	96.06 (0)	594.88 (0)	211.94 (0)	529.95 (0)	197.46 (0)
Exp, $V = 0.1$	107.2 (0)	516.73 (0)	234.19 (0)	460.11 (0)	195.15 (0)
Exp, $V = 0.01$	61.01 (0)	213.45 (0)	170.67 (0)	192.4 (0)	123.44 (0)
Exp, $V = 0.001$	32.41 (0.001)	34.93 (0)	34.95 (0)	34.69 (0)	34.11 (0)
1-hop neighbor	2.28 (0.011)	10.22 (0)	5.43 (0)	9.2 (0)	4.85 (0)
2-hop neighbor	1.87 (0.032)	12.67 (0)	8.59 (0)	11.66 (0)	6.11 (0)

**Table 1: Standardized Moran’s I statistics for the Chicago bikeshare data, with permutation test  $p$ -values in parentheses.**

Feature pair	No ESF	ESF-BIC	ESF-AIC
%AA vs. No. of stations	<b>0.007</b>	0.27	0.35
Med. Inc. vs. No. of stations	<b>4.4e-16</b>	0.999	0.99
%AA vs. Med. Inc.	<b>5.8e-129</b>	<b>2.6e-5</b>	<b>1.3e-8</b>

**Table 2: Pairwise  $p$ -values from asymptotic correlation tests with and without ESF. Bold indicates significant evidence of rejecting null (at level 0.05).**

- [8] Sam Corbett-Davies and Sharad Goel. 2018. The measure and mismeasure of fairness: A critical review of fair machine learning. *arXiv preprint arXiv:1808.00023* (2018).
- [9] Cyrus DiCiccio, Sriram Vasudevan, Kinjal Basu, Krishnaram Kenthapadi, and Deepak Agarwal. 2020. Evaluating Fairness Using Permutation Tests. In *Proceedings of the 26th ACM SIGKDD International Conference on Knowledge Discovery & Data Mining*. 1467–1477.
- [10] Stéphane Dray, Pierre Legendre, and Pedro R. Peres-Neto. 2006. Spatial modelling: a comprehensive framework for principal coordinate analysis of neighbour matrices (PCNM). *Ecological Modelling* 196, 3 (2006), 483 – 493.
- [11] EEOC. 1979. Questions and Answers to Clarify and Provide a Common Interpretation of the Uniform Guidelines on Employee Selection Procedures. (1979). <https://www.eeoc.gov/laws/guidance/questions-and-answers-clarify-and-provide-common-interpretation-uniform-guidelines>.
- [12] Anna Goodman and James Cheshire. 2014. Inequalities in the London bicycle sharing system revisited: impacts of extending the scheme to poorer areas but then doubling prices. *Journal of Transport Geography* 41 (2014), 272–279.
- [13] D. Griffith. 2004. A Spatial Filtering Specification for the Autologistic Model. *Environment and Planning A* 36 (2004), 1791 – 1811.
- [14] Daniel A Griffith. 2004. A Spatial Filtering Specification for the Autologistic Model. *Environment and Planning A: Economy and Space* 36, 10 (2004), 1791–1811.
- [15] Daniel A. Griffith, Yongwan Chun, and Bin Li. 2019. *Spatial Regression Analysis Using Eigenvector Spatial Filtering*. Academic Press.
- [16] Mark F Guagliardo. 2004. Spatial accessibility of primary care: concepts, methods and challenges. *International journal of health geographics* 3, 1 (2004), 3.
- [17] S. Heath. 2021. *COVID-19 Vaccine Poses Geographic Care Access Health Disparities*. <https://billypenn.com/2021/03/18/philadelphia-vaccine-registry-equity-internet-access-walkup-fema-site/>
- [18] Cheng Jin, Jianquan Cheng, Yuqi Lu, Zhenfang Huang, and Fangdong Cao. 2015. Spatial inequity in access to healthcare facilities at a county level in a developing country: a case study of Deqing County, Zhejiang, China. *International journal for equity in health* 14, 1 (2015), 1–21.
- [19] Y. Lee and E. L. Ogburn. 2020. Testing for Network and Spatial Autocorrelation. In *NetSci-X 2020*. 91–104.
- [20] M. Marin. 2021. *Philly vaccine interest registry has built-in disparities, widening the racial divide*. <https://billypenn.com/2021/03/18/philadelphia-vaccine-registry-equity-internet-access-walkup-fema-site/>
- [21] N. Mehrabi, F. Morstatter, N. Saxena, et al. 2019. A Survey on Bias and Fairness in Machine Learning. *arXiv:1908.09635*.
- [22] Patrick AP Moran. 1950. Notes on continuous stochastic phenomena. *Biometrika* 37, 1/2 (1950), 17–23.
- [23] NACTO. 2015. Walkable Station Spacing is Key to Successful, Equitable Bike Share. (2015).
- [24] Flora Ogilvie and Anna Goodman. 2012. Inequalities in usage of a public bicycle sharing scheme: socio-demographic predictors of uptake and usage of the London (UK) cycle hire scheme. *Preventive medicine* 55, 1 (2012), 40–45.
- [25] K. A. O’Neil and R. A. Redner. 1993. Asymptotic distributions of weighted ustatistics of degree 2. *Ann. Probab.* 21 (1993), 1159–1169.

- [26] A. SenGupta. 2007.  $P^3$  approach to intersection–union testing of hypotheses. *J. Stat. Plan. Inf.* 137 (2007), 3753–3766.
- [27] Hajime Seya, Daisuke Murakami, Morito Tsutsumi, and Yoshiki Yamagata. 2015. Application of LASSO to the Eigenvector Selection Problem in Eigenvector-based Spatial Filtering. *Geographical Analysis* 47, 3 (2015), 284–299.
- [28] C. P. Shapiro and L. Hubert. 1979. Asymptotic normality of permutation statistics derived from weighted sums of bivariate functions. *Ann. Statist.* 7 (1979), 788–794.
- [29] A. Williams and A. Emamdjomeh. 2018. *America is more diverse than ever—but still segregated*. <https://www.washingtonpost.com/graphics/2018/national/segregation-us-cities/>